Supplementary Methods

Immunoblot identification of anti-LCP1 IgG

Purified recombinant LCP1 recombinant protein (OriGene, Rockville, MD) or tetanus toxin (Sigma, St Louis, MO) was electrophoretically separated by SDS-PAGE and subsequently transferred to nitrocellulose membranes according to conventional methodology. After blocking, membranes were cut into strips and probed with 1:100 human sera in blocking buffer overnight. Human IgG was interrogated by anti-human IgG-HRP #2040-05 (Southern Biotech, Birmingham, AL). Data were collected onto autoradiography film using chemiluminescent detection reagent according to standard protocols.

Supplementary Tables

Supplementary Table 1: CLL patient clinical statistics. Patient identifier correlates to samples utilized in Figure 2. Statistics including gender, white blood cell count (WBC) at date of blood draw, cytogenetic abnormalities, prior therapies, age and Rai stage at diagnosis are provided. Key: ND = not done, FR = Fludarabine + Rituximab, F = Fludarabine, FCR = Fludarabine + Cyclophosphamide + Rituximab, PCR = Pentostatin + Cyclophosphamide + Rituximab, A = Alemtuzumab, Chl = Chlorambucil, HDMP+R = high dose solumedrol + Rituximab, Len = Lenalidomide.

Supplementary Figure Legends

Supplementary Figure 1: Oncomine microarray analysis of CLL cells and healthy B cells demonstrates higher LCP1 expression in leukemia. Statistical analysis found by Student's T-test; Error bars s.e.m.

Supplementary Figure 2: A) Immunoblot demonstrated that 15 of 22 CLL patients and 5 of 8 healthy donors had detectable serum LCP1 specific IgG. B) In contrast, 100% of healthy donors had detectable serum responses to tetanus toxin; meanwhile, only a small percentage of CLL patients, most of which had received intravenous immunoglobulin (IVIG), were responsive to tetanus. Positive control blots were probed with LCP1 specific monoclonal antibody and the appropriate HRP-linked secondary antibody, and negative control blots were only probed with secondary HRP linked anti-human IgG.

Supplementary Figure 3: A) Oncomine microarray data reveals high level LCP1 mRNA expression in leukemia and lymphoma cell lines as compared to healthy non-hematopoietic tissues (grey). B) Oncomine mRNA analysis of primary tumors reveals constitutive expression of LCP1 in CLL as well as other leukemias, lymphomas, and a subset of prostate cancers.

Supplementary Figure 4: CB17/SCID mice were engrafted with $1X10^7$ live 697, 697-Empty Vector (top row), or 697 LCP1-knockdown (middle row) cells and sacrificed on day 18. Bone marrow infiltration of GFP+human-CD19+ cells was quantified by flow cytometry. Outgrowth of vector negative 697 cells is indicated by CD19+GFP- gating.

B) H&E stained sections of femoral bone marrow from 697-Empty Vector (left) demonstrate infiltration and replacement of normal bone marrow with neoplastic lymphocytes as compared to sections from 697-LCP1 shRNA (right) which depict hematopoietic bone marrow consistent with non engrafted control mice.

Supplementary Table 1

Patient	Gender	IgVH	WBC	Cytogenetics	Age	Rai at Dx	Prior Therapy
CLL-A	F	unmut	36.2	11q	80	0	FRx6
CLL-B	M	mut	18.3	13q	65	I	FRx6, Len
CLL-C	M	unmut	24.1	ND	63	0	FRx2
CLL-D	F	mut	67.5	13q	48	I	PCRx2, Len
CLL-E	M	ND	24.5	13q	73	II	Fx2, FCRx3, PCR, R, A, CDK, HDMP+R, Len
CLL-F	M	mut	46.7	13q	73	I	Chl, F, FRx6, Len
CLL-G	F	unmut	23.5	11q, 17p, tri-12	77	I	A, Len
CLL-H	F	unmut	97.7	tri-12	67	II	FRx2, Rx10, Len

Supplementary Figure 1

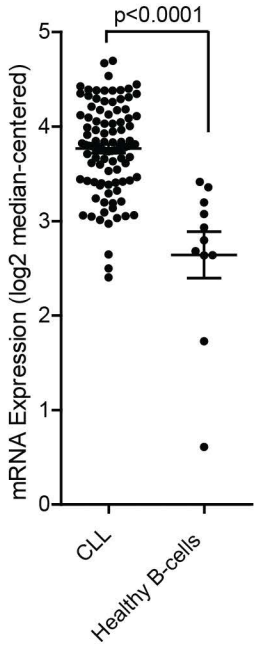

Supplementary Figure 2

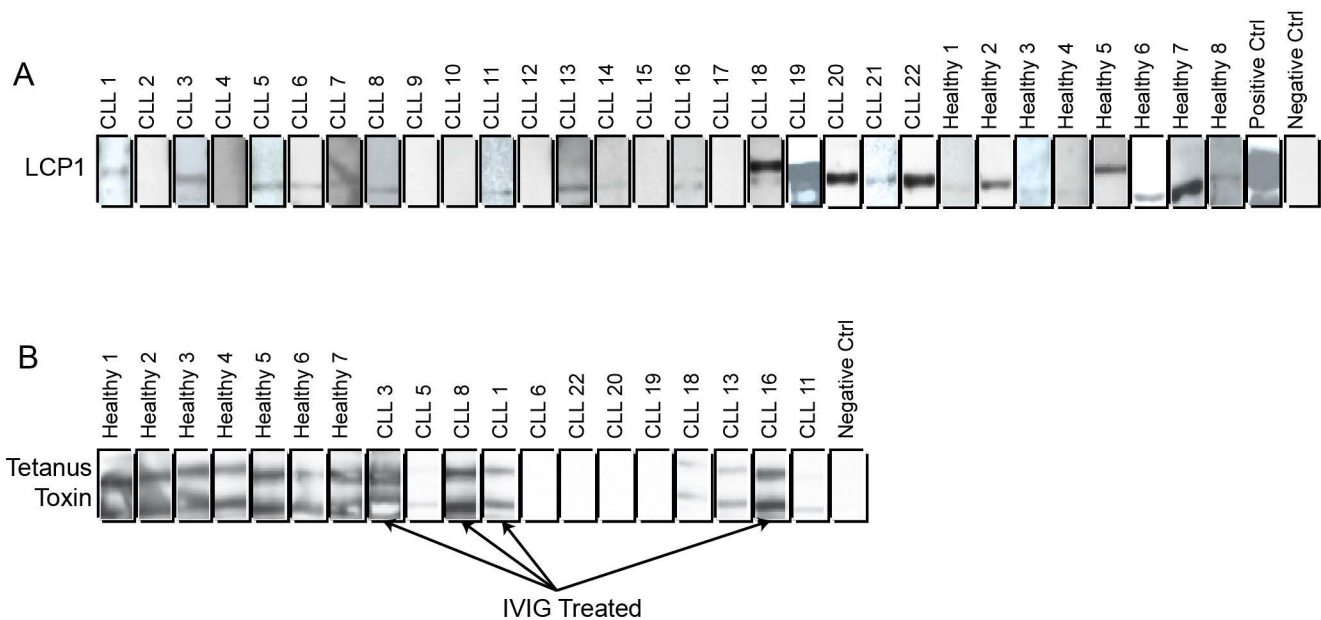

Supplementary Figure 3

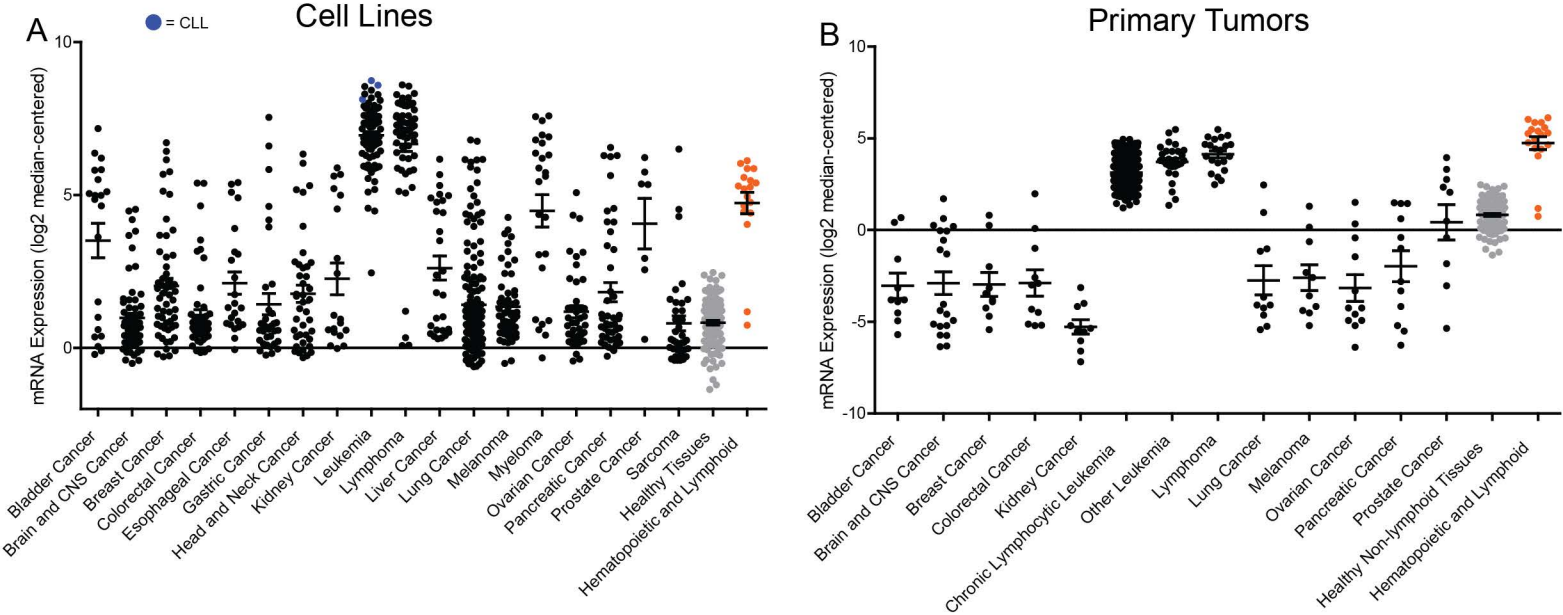

Supplementary Figure 4